Gene 818 (2022) 146226

Contents lists available at ScienceDirect

Gene

journal homepage: www.elsevier.com/locate/gene

Transcriptome analysis based on dietary beta-carotene supplement reveals genes potentially involved in carotenoid metabolism in *Crassostrea gigas*

Sai Wan [a], Qi Li [a,b,*], Hong Yu [a], Shikai Liu [a], Lingfeng Kong [a]

[a] Key Laboratory of Mariculture, Ministry of Education, Ocean University of China, 5 Yushan Road, Qingdao 266003, China
[b] Laboratory for Marine Fisheries Science and Food Production Processes, Qingdao National Laboratory for Marine Science and Technology, Wenhai Road, Qingdao 266237, China

ARTICLE INFO

Edited by Xavier Carette

Keywords:
Crassostrea gigas
Carotenoids
Transcriptome sequencing
Retinoid homeostasis
Carotenoid oxygenase
Candidate genes

ABSTRACT

Carotenoids are essential micronutrients for animals, and they can only be obtained from the diet for mollusk as well as other animals. In the body, carotenoids undergo processes including absorption, transport, deposition, and metabolic conversion; however, knowledge of the involved genes is still limited. To elucidate the molecular mechanisms of carotenoid processing and identify the related genes in Pacific oyster (*Crassostrea gigas*), we performed a comparative transcriptome analysis using digestive gland tissues of oysters on a beta-carotene supplemented diet or a normal diet. A total of 718 differentially expressed genes were obtained, including 505 upregulated and 213 downregulated genes in the beta-carotene supplemented group. Function Annotation and enrichment analyses revealed enrichment in genes possibly involved in carotenoid transport and storage (e.g., LOC105342035), carotenoid cleavage (e.g., LOC105341121), retinoid homeostasis (e.g., LOC105339597) and PPAR signaling pathway (e.g., LOC105323212). Notably, down-regulation of mRNA expressions of two apolipoprotein genes (LOC105342035 and LOC105342186) by RNA interference significantly decreased the carotenoid level in the digestive gland, supporting their role in carotenoid transport and storage. Based on these differentially expressed genes, we propose that there may be a negative feedback mechanism regulated by nuclear receptor transcription factors controlling carotenoid oxygenases. Our findings provide useful hints for elucidating the molecular basis of carotenoid metabolism and functions of carotenoid-related genes in the oyster.

1. Introduction

Carotenoids are widely distributed pigments with an orange-red color and consist of more than 1100 members (Yuan et al., 2015; Yabuzaki, 2017). They can be synthesized by many plants, bacteria, and fungi, but not by animals with few exceptions (Moran and Jarvik, 2010), so diet is the only carotenoid source. Carotenoids are of physiological importance in various aspects of animal life. One the one hand, intact carotenoids accumulated in animal tissues may act as antioxidants or signal pigments involved in body coloration (Toews et al., 2016). On the other hand, they were precursors of vitamin A and other carotenoid derivatives playing essential roles in vision (Kiser et al., 2014) and modulating cell differentiation, embryonic development, immunity, and metabolism (Hall et al., 2011; Blaner, 2019; Li et al., 2020).

After intake by animals, carotenoids were released from food matrix, incorporated into lipid droplets and absorbed in the intestine. Then they were transported, transformed, cleaved or deposited in tissues. These processes have been shown to be influenced by various external factors such as food source, seasonal changes (Olsen et al., 2005; Chimsung et al., 2013) and light cycle (Tan et al., 2021b). However, genetic factors were also considered to play a crucial role in mechanisms underlying carotenoid processing (Toews et al., 2017).

In particular, in recent years, carotenoid-based animal coloration has been the focus of genetic function and evolutionary studies concerning the establishment and maintenance of these carotenoid-dependent traits (Toews et al., 2017). Various genes underlying these traits were reported

Abbreviations: PPAR, peroxisome proliferator activated receptor; SRB, scavenger receptor class B; CCO, carotenoid cleavage oxygenase; RAR, retinoic acid receptor; RXR, retinoid X receptor; TCC, total carotenoid content; FDR, false discovery rate; DEG, differentially expressed genes; LPD-N, lipoprotein N-terminal domain; EGFP, enhanced green fluorescent protein; qPCR, quantitative reverse transcription PCR; FPKM, fragments per kilobase per million mapped reads; DBD, DNA binding domain; LBD, ligand binding domain; RDH, retinol dehydrogenase.

* Corresponding author at: Key Laboratory of Mariculture, Ministry of Education, Ocean University of China, 5 Yushan Road, Qingdao 266003, China.
E-mail address: qili66@ouc.edu.cn (Q. Li).

https://doi.org/10.1016/j.gene.2022.146226
Received 4 October 2021; Received in revised form 18 December 2021; Accepted 13 January 2022
Available online 19 January 2022

to involved in selective deposition, enzymatical conversion and cleavage of specific types of carotenoids (Maoka, 2009). For instance, some members of scavenger receptor class B (SRB) genes, encoding for lipoprotein receptors, are important for the cellular uptake of carotenoids (Kiefer et al., 2002; Toews et al., 2017). Similarly, Cameo2 and SCRB15 are involved in the selective transport of lutein and beta-carotene to the silk gland, which is responsible for cocoon coloration in *Bombyx mori* (Sakudoh et al., 2010; Sakudoh et al., 2013). Furthermore, genomic and biochemical analyses with yellow and red feather canaries (Toomey et al., 2017) revealed a role for the high-density lipoprotein receptor SCARB1 in cellular uptake of carotenoids, responsible for carotenoid-based coloration. In terms of carotenoid cleavage and elimination, carotenoid cleavage oxygenases (CCOs), an evolutionary conserved cytosolic enzyme, were shown to be key players (Poliakov et al., 2017). The *cis*-acting regulatory mutations in BCDO gene result in more uncleaved carotenoids in yellow-skinned chickens compared to white-skinned ones (Eriksson et al., 2008).

It was noteworthy that research have shown that mammals have evolved efficient mechanisms to control carotenoid homeostasis, which include at least a negative feedback control mechanism implemented by carotenoid oxygenases that control intestinal carotenoid absorption to adapt to fluctuations in dietary availability of these lipids (Lobo et al., 2010; von Lintig, 2010). Within these feedback regulation loops, nuclear receptor transcription factors, including peroxisome proliferator-activated receptors (PPARs) (Boulanger et al., 2003; Malerød et al., 2003), retinoic acid receptor (RAR) and retinoid X receptor (RXR) (Xiao et al., 1995), as well as intestinal transcription factor (ISX) (Lobo et al., 2010), can regulate the expression of genes involved in carotenoid metabolism, which are essential components of carotenoid and retinoid (i.e., carotenoid derivatives) homeostasis (Andre et al., 2014). Other genes, such as Niemann Pick C1-like 1 (NPC1L1) (During et al., 2005), ATP-binding cassette sub-family G member 5 (ABCG5) (Herron et al., 2006), CYP2J19 (Lopes et al., 2016; Mundy et al., 2016; Twyman et al., 2016) also play roles in carotenoid transport and binding.

Like other animals, mollusks acquire a variety of carotenoids from their diet, i.e. microalgae filtered from seawater. Most of these carotenoids are fucoxanthin, diatoxanthin, diadinoxanthin, and alloxanthin and their metabolites (Maoka, 2009; Maoka, 2011). Recent multi-omic and biochemical analyses in mollusk species, focusing on mining genes for carotenoid-based coloration of shells and tissues, have identified candidate genes underlying molecular mechanisms responsible for these traits. For instance, in bivalves, studies in Yesso scallop *(Patinopecten yessoensis)* named 'Haida golden scallop' with orange adductor muscle revealed that the orange color is caused by carotenoid deposition (Li et al., 2010). Subsequently, genes encoding the stearoyl-CoA desaturase (SCD) (Li et al., 2015), lysophosphatidylcholine acyltransferase 1 (LPCAT1) (Wang et al., 2015) and several proteins (Zhang et al., 2014) were identified as candidates related to carotenoid accumulation. At last, carotenoid accumulation was shown to be the result of *PyBCO-like 1* down-regulation (Li et al., 2019). Meanwhile, bay scallop *Argopecten irradians* (Song and Wang, 2019) and noble scallop *Chlamys nobilis* (Liu et al., 2015) also exhibited carotenoid-based shell color and tissue color, and the underlying genes, such as apolipophorin and SRB, were identified by transcriptomic and/or proteomic analyses. Using a similar strategy, genes enriched in phototransduction and rhodopsin related Gene Ontology (GO) terms were identified to be associated with higher total carotenoid content (TCC) in yellow shell pearl oysters *Pinctada fucata martensii* compared with black shell ones (Xu et al., 2019). In addition, through correlation analyses between gene expression and total carotenoid content in purple and white inner-shell color pearl mussel *Hyriopsis cumingii*, Li et al., (2014) found a novel *hcApo* gene that may be responsible for higher TCC in multiple tissues (Li et al., 2014).

The Pacific oyster *Crassostrea gigas* is a widely distributed and economically important species that is rich in carotenoids. They accumulate various carotenoids from their dietary microalgae and may modify them by metabolic reactions and deposit metabolites in tissues (Maoka, 2011). Considering the largest production of *C. gigas* among all cultured aquatic animals (FAO, 2016) and the seasonal fluctuations in their intake of carotenoid-rich microalgae, it is important to better understand the molecular mechanisms of carotenoid metabolism in Pacific oyster, from the economy, animal breeding, gene function and evolution perspectives (Shahidi et al., 1998; Hubbard et al., 2010);

In the present study, to investigate the molecular mechanisms of carotenoid processing in *C. gigas*, we first identified genes potentially involved in carotenoid transport and storage by comparative transcriptome analysis, with the role of two lipoprotein genes (LOC105342035 and LOC105342186) being further supported by RNAi assays. Secondly, based on the differentially expressed genes, we inferred the existence of a diet-responsive negative feedback mechanism in *C. gigas*, regulated mainly by nuclear receptor transcription factors controlling carotenoid cleavage enzyme gene expressions and retinoid production. Our findings provide valuable information for further research on the mechanisms of carotenoid metabolism.

2. Materials and methods

2.1. Ethics statement

The Pacific oysters used in this study were cultured by us, and we are allowed to use these materials for research. All experiments on them were carried out in accordance with institutional and national guidelines. Since no endangered or protected species were involved in our experiments, no specific permission was required for the experiment materials.

2.2. Experimental animals

One-year old Pacific oysters (6.64 ± 0.65 cm in shell height and 16.39 ± 4.30 g in total weight) were collected in September 2020 from Rushan, Shandong, China. During the acclimation period, all the oysters were cultured at 12–15 °C for 10 days in aerated seawater, which was renewed every other day. Oysters were fed twice a day using *Chlorella vulgaris*, with the daily amount of 300 million algal cells per oyster, to satiate them (Kuhn et al., 2013).

2.3. Beta-carotene feeding experiment

In the formal experiment, 160 oysters were cultured in 10 tanks, each containing 50 L seawater, and were divided into two groups, including the beta-carotene supplemented group (group caro) and the control group (group ctrl). Each group contained five replicates, with 16 oysters in each replicate. All culture conditions were the same as during the acclimation period, except that oysters in group caro were fed with additional beta-carotene. As beta-carotene is insoluble in water, water-soluble microencapsulated beta-carotene was purchased from LTD Xinhe Biotech (Hubei, China) and well mixed with *Chlorella vulgaris* algae for the experiment as previously reported in *Hyriopsis cumingii* (Chen et al., 2019). Considering beta-carotene content of 1% (w/w) in the microcapsules, each oyster was fed with 0.28 g of microencapsulated beta-carotene per day (i.e., 2.8 mg of pure beta-carotene). The beta-carotene microcapsules used are lipid-based and their lipophilic shells consist mainly of triglyceride oil and a small amount of surface active materials (Lin et al., 2018).

After 30 days of cultivation, 9 oysters were randomly sampled from each group. The digestive gland tissue from every oyster was dissected, immediately frozen in liquid nitrogen, and then stored at −80 °C for total RNA extraction.

2.4. RNA isolation, library preparation, and sequencing

Total RNA of digestive gland tissues from eighteen oysters (i.e., nine from beta-carotene group and nine from control group) were extracted

separately using TRIZOL, assessed by electrophoresis on 1% agarose gel for quality and quantified using NanoPhotometer® spectrophotometer (IMPLEN, CA, USA). RNA concentration and integrity were determined using Qubit® RNA Assay Kit in Qubit® 2.0 Flurometer (Life Technologies, CA, USA) and the RNA Nano 6000 Assay Kit of the Bioanalyzer 2100 system (Agilent Technologies, CA, USA), respectively. For each group, three libraries were constructed and each one consists of equal amounts of total RNA pooled from three replicates. For comparison, total RNA (3 μg per sample, 1 μg per individual) from oysters of both groups was used to prepare six pair-end cDNA libraries. Briefly, ribosomal RNA (rRNA) was firstly depleted from the total RNA by using Epicentre Ribo-zero™ rRNA Removal Kit (Epicentre, USA), and then cleaned up by ethanol precipitation.

Sequencing libraries were subsequently generated with the rRNA-depleted RNA by NEBNext® Ultra™ Directional RNA Library Prep Kit for Illumina® (NEB, USA) following manufacturer's recommendations. In this process, libraries were fragmented using divalent cations under elevated temperature in NEBNext First Strand Synthesis Reaction Buffer (5X). And then first strand cDNA was synthesized using random hexamer primer and M-MuLV Reverse Transcriptase (RNaseH-), followed by RNA degradation and second strand cDNA synthesis with RNase H and DNA Polymerase I, in which dNTPs with dTTP were replaced by dUTP. Remaining overhangs were converted into blunt ends via exonuclease/polymerase activities. Subsequently, 3′ ends of DNA fragments were adenylated and ligated with NEBNext Adaptor with hairpin loop structure to prepare for hybridization. Then 350–400 bp cDNA fragments were selected with AMPure XP system (Beckman Coulter, Beverly, USA). Before PCR, USER Enzyme (NEB, USA) was used to degrade the second-strand cDNA containing dUTP. Then PCR was performed with Phusion High-Fidelity DNA polymerase, Universal PCR primers and Index (X) Primer. After the purification of PCR products with AMPure XP system, library quality was assessed on the Agilent Bioanalyzer 2100 system. After library generation, the clustering of all samples was conducted on a cBot Cluster Generation System using TruSeq PE Cluster Kit v3-cBot-HS (Illumia) according to the manufacturer's instructions. At last, the resulting libraries were sequenced using 150 bp paired-end reads on an Illumina NovaSeq 6000 platform. Sequence read data have been deposited at the NCBI sequence read archive (SRA) under the accession number PRJNA765831 (Table S1).

2.5. Quality control, mapping and gene expression calculation

Raw sequence data from the 6 libraries were quality trimmed using fastp v0.20.1 package (Chen et al., 2018) to obtain clean reads removed adapter sequences, poly-N sequences, and low quality reads, and to produce reports of the Q20, Q30, and GC content of the clean data. All the downstream analyses were based on these high-quality clean data.

Then, all the RNA-seq reads were mapped to the oyster genome (GenBank accession No. GCA_902806645.1) with the HISAT2 (Kim et al., 2015) (v2.2.1, with following parameters -rna-strandness RF and -dta options). The produced SAM files were converted to BAM files and sorted by SAMtools v1.10 (Li et al., 2009). On the basis of the C. gigas genome sequence, transcript assembly was performed by StringTie v2.1.2 (Pertea et al., 2015), with which StringTie estimated expression abundance for input to IsoformSwitchAnalyzeR v1.13.05 (Vitting-Seerup and Sandelin, 2019). Then, raw read counts of all genes were extracted with the IsoformSwitchAnalyzeR and the fragments per kilobase per million mapped reads (FPKM) of each gene was also calculated.

2.6. Differential expression analysis, gene annotation and GO and KEGG enrichment analysis

Differentially expressed genes (DEGs) based on read counts was identified with the R package DESeq2 v1.30.1 (Wang et al., 2010), with a model based on a negative binomial distribution and adjustment of *p*-values using the Benjamini and Hochberg approach for controlling false discovery rate (FDR). The resulting adjusted *p*-values < 0.05 and $|\log2FoldChange| > 1$ were used to find differentially expressed genes. Further, isoform usage, nucleotide and amino acid sequences of differentially expressed genes (DEGs) were deduced using IsoformSwitchAnalyzeR.

To establish the latest local protein databases of Gene ontology (GO) (Khatri and Draghici, 2005) and Kyoto Encyclopedia of Genes and Genomes (KEGG) (Kanehisa et al., 2008), all the metazoan protein sequences with GO numbers were download from NCBI protein database, and those with K numbers were obtained through KEGG API (https://www.kegg.jp/kegg/rest/keggapi.html). Through BLASTP (cut-off E-value of 1e-5) against the resulting databases, deduced amino acid sequences of all the genes (FPKM > 1 in at least one group) were assigned with GO and KEGG numbers. GO and Kegg enrichment was done using clusterProfiler (Yu et al., 2012) with default parameters and then visualized.

2.7. Quantitative real-time PCR validation of DEGs

For validation of RNA-seq, a total of 16 DEGs of insterest were selected. With the remaining total RNA for RNA-seq, cDNAs of six samples were synthesized, using a HiScript III RT SuperMix for qPCR (+gDNA wiper) kit (Vazyme, Nanjing, China). Specific primers for qRT-PCR were designed with Primer-Blast at NCBI (Ye et al., 2012) (Table S2). Enlongation Factor was used as an internal controls (Renault et al., 2011).

qRT-PCR assays were performed on a Roche LightCycler 480 Real-time PCR System (Roche, Switzerland) using EvaGreen 2x qPCR MasterMix-No Dye (ABM). Reactions (20 μl) contained cDNA (4 μl, diluted 1:15 in water), MasterMix (10 μl), forward primer (3 μl, 2 μM) and reverse primer (3 μl, 2 μM). Amplification procedures were as following: pre-incubation at 94 °C for 10 min, followed by 40 cycles of 15 s at 95 °C, 1 min at 60 °C, and a final melting curve step was conducted to verify that each primer set amplified a single product. Two technical replicates were performed for each sample, and six samples were used as biological replicates. The qPCR results were analyzed using Real-time PCR Miner (http://www.miner.ewindup.info/) (Zhao and Fernald, 2005), with which PCR efficiencies and optimal cycle threshold (Ct) values were estimated. The gene expression was quantified by normalizing to Enlongation Factor gene expression.

2.8. Sequence analysis and phylogenetic analysis of genes of interest

Differentially expressed genes encoding apolipoproteins, carotenoid oxygenase, nuclear receptor transcription factors were chosen for further sequence analyses. Their mRNAs, ORFs and proteins were downloaded from the the National Center for Biotechnology Information (NCBI) and deduced from the transcriptome data using IsoformSwitchAnalyzeR (Protein sequences: File S1).

Conserved protein domains were predicted with the Simple Modular Architecture Research Tool SMART (http://smart.embl-heidelberg.de/) (Letunic et al., 2021). The amino acid (aa) sequences of apolipoprotein genes and carotenoid oxygenase of *C. gigas*, as well as homologous genes of other species retrieved from NCBI were aligned with MAFFT v7.471 (Katoh et al., 2002) alignment software using the L-INS-I algorithm and visualized in Jalview (Waterhouse et al., 2009). Their phylogenetic trees were constructed by the Maximum-Likelihood (ML) algorithm using IQ-Tree 1.4.3 (Minh et al., 2013), and the topological stability of the trees was evaluated by 1000 bootstrapping replicates.

2.9. RNA interference (RNAi) experiment of apolipoprotein genes

Based on differential expression analysis and functional enrichment analysis, we selected two apolipoprotein genes (LOC105342035 and LOC105342186), designated *CgApo1* and *CgApo2* respectively, for further RNA interference experiment to analyse their function. Through

sequence analysis and alignment, we found a shared conserved domain called lipoprotein N-terminal domain (LPD-N) between CgApo1 and CgApo2 (Fig. 1a), whose nucleotide sequences were highly similar (99.88%; Fig. S1) and chosen as candidate target region of dsRNA. The cDNA of the two CgApo genes was synthesized and used as template for PCR amplification with Phanta® Max Super-Fidelity DNA Polymerase (Vazyme), and primers were designed with Primer-Blast (Table S2). After purification, the PCR products were used as templates and amplified with the primers containing T7 promoter. For a control group, a DNA fragment of enhanced green fluorescent protein (EGFP) gene was also cloned using specific primers with T7 promoters (Table S2).

After purification, the PCR products were used as templates for in vitro transcription using a T7 RNAi Transcription Kit (Vazyme) according to the manufacturer's instructions. The quality of obtained dsRNA was assessed by electrophoresis on 1% agarose gel and quantified with a NanoDrop 2000 spectrophotometer (Thermo Fisher Scientific, USA), after which dsRNA was diluted to 1 μg/μl with PBS and dispensed into tubes (100 μl per tube).

Prior to dsRNA injection, oysters with an average shell height of 80 mm were subject to one week starvation to consume stored carotenoids. Then, a total of 54 individuals were randomly separated into three groups consisting of dsCgApo, dsEGFP and phosphate buffered saline (PBS) group. The oyster shells were ground with an electric drill to create a slit approximately 1-cm wide at the shell edges near the adductor muscle for subsequent injection into the muscle. Oysters in the RNAi group were injected with 100 μl of prepared dsRNA for CgApo genes. Besides, the same amount of dsRNA for EGFP and the same volume of PBS were also injected into adductors of oysters in the negative

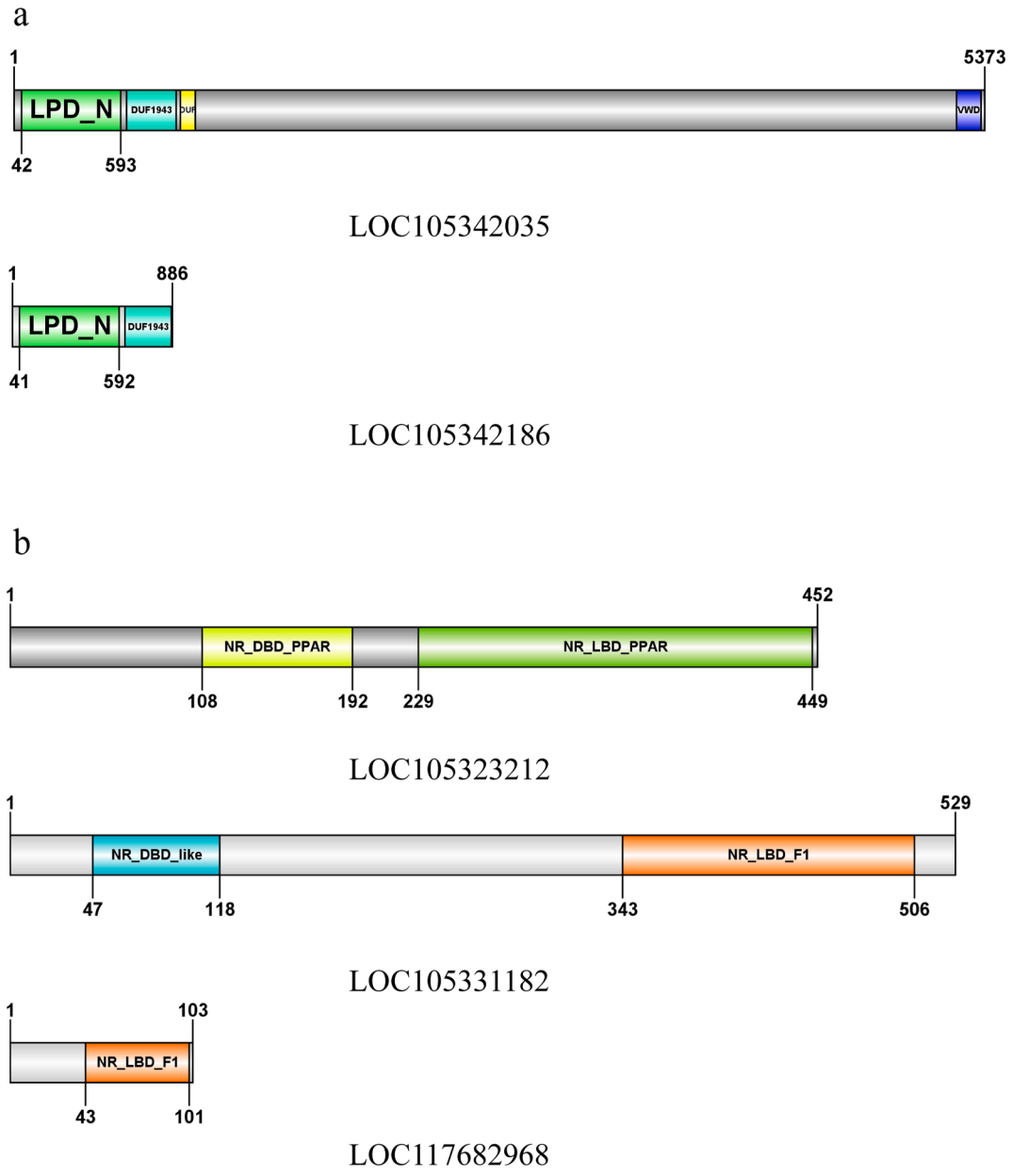

Fig. 1. Protein organization of differentially expressed apolipoproteins and nuclear receptors. a. apolipoproteins: LOC105342035 and LOC105342186; nuclear receptors: LOC105323212, LOC105331182 and LOC117682968; Arabic numbers: position and length for protein (aa). LPD_N: Lipoprotein N-terminal Domain (Accession: smart00638); DUF1943: Domain of unknown function (pfam09172); VWD: von Willebrand factor type D domain (smart00216); b. nuclear receptors: LOC105323212, LOC105331182 and LOC117682968; NR_DBD_PPAR: DNA-binding domain of peroxisome proliferator-activated receptors (cd06965); NR_LBD_PPAR: The ligand binding domain of peroxisome proliferator-activated receptors (cd06932); NR_DBD_like: DNA-binding domain of nuclear receptors (cd06916); NR_LBD_F1: Ligand-binding domain of nuclear receptor family 1 (cd06929);

control and empty group, respectively.

One day after injection, oysters were fed normally as mentioned above; two days later, they were injected again with those dsRNA or PBS. The RNAi experiment lasted for 8 days. At last, digestive glands of survived oysters in dsCgApo (n = 13), dsEGFP (n = 14) and PBS (n = 10) group were collected and frozen immediately in liquid nitrogen. All samples were stored at −80 °C until RNA and carotenoid extraction. RNAi efficiency was determined by qPCR.

2.10. Effect of dsRNA on target mRNA and total carotenoid content (TCC) in the digestive gland

For every individual, half of the digestive gland was used for RNA extraction and the other half for carotenoid extraction. qPCR was performed as described above with two technological replicates for each sample.

Prior to carotenoid extraction, digestive glands from about five oysters were mixed and dried in a freeze-dryer (SCIENTZ-10 N, Ningbo Scientz Biotechnology CO., China) for 24 h, and ground with pestles and mortars that sterilised at 180 °C. Total carotenoids were extracted according to Zheng's method (Yanar et al., 2004) with minor modification. Every sample was homogenized and dissolved in 5 ml acetone, followed by shaking at 200 rpm for 3 h at 25 °C in an aphotic environment of a temperature control shaking incubator. After centrifuging the extracts at 5000 rpm for 5 min, the supernant was passed through a 0.22 μm syringe filter. Then the concentration of the total carotenoid was determined by an ultraviolet–visible spectrophotometer (UNICO UV-2800A, China) at 480 nm and calculated with the following formula: TCC (%) = (A480 × V × 10000)/(1900 × w), where A480 is the absorbance of the sample at 480 nm, V is the diluted volume of the sample (ml), 1900 is the extinction coefficient of 1% (g/ml) carotenoids in acetone in a 1 cm cuvette at 480 nm, W is the sample dry weight of tissue powder (g).

2.11. Statistical analysis

Data are shown as mean ± SD. Two-group comparison analyses were performed using unpaired two-tailed *t*-test for qPCR validation. TCC and qPCR data were compared among groups with one-way ANOVA. Results were considered significant at $^{*}P < 0.05$ and $^{**}P < 0.01$.

3. Results

3.1. Sequencing and mapping of RNA-Seq libraries

To identify differently expressed genes between oysters fed on the beta-carotene supplemented diet and normal diet, six cDNA libraries constructed from the digestive gland of two groups of oysters (group caro and ctrl) were sequenced using Illumina NovaSeq 6000, and the read data were submitted to the NCBI SRA database. After quality control, a total of 503.8 million (M) clean reads were obtained from 506.3 M pair-end 150 bp raw reads of six libraries, with the resulting total reads length of 75.45 Giga base (G) and Q20 (%) of each sample varying from 98.42% to 98.58% (Table S1). The filtered high-quality reads of each sample were aligned to the *C. gigas* genome, resulting in overall alignment rates varying from 78.77% to 80.80%.

The abundance of all genes (42,838) was normalized and calculated by FPKM. The distribution of gene expressions showed similar patterns among libraries, and genes with FPKMs > 1 accounted for about 44% of the total number (Fig. S2).

3.2. Differential expression analysis and validation by qRT-PCR

Genes with FPKMs less than 1 were considered low abundance genes and omitted. The DEGs between the beta-carotene supplemented group and the control group were identified by DESeq2 with adjusted *P* value < 0.05 and |log2 (fold change)| > 1. As a result, 718 DEGs were found, in which 505 genes (~70.33%) were up-regulated and 213 (~29.67%) genes down-regulated in the group caro compared with group ctrl (Fig. S3; Fig. S4). Genes of special interest were shown in Fig. 2.

Sixteen genes of interest were chosen to perform qPCR, and the obtained values of log2FC were compared with those from the RNA-seq data. Especially, carotenoid oxygenase genes (LOC105321989 and LOC117690758) with no different expression in transcriptome data were further validated. The results showed that most genes analyzed by qPCR share same expression patterns with those obtained from the RNA-seq data, especially including apolipoprotein genes, carotenoid oxygenase genes and nuclear receptor genes that we focused on (Fig. S5).

3.3. Gene annotation and enrichment analysis of DEGs

In order to analyze functions of the DEGs between group caro and ctrl, these genes were annotated and enriched with GO and KEGG database. The significantly enriched GO terms for biological process at level 5 are illustrated in Fig. 3. The detailed results for three main GO categories (biological process, cellular component and molecular function) are listed in Table S3. A total of 49 KEGG pathways were significantly enriched and sorted by the number of genes in Fig. 4 and details were listed in Table S4. Furthermore, all the genes involved in enriched terms or pathways were annotated with description from GO and KEGG database (Table S5).

In general, results of GO and KEGG enrichment analysis were similar. Except for xenobiotic metabolic related terms that may be caused by microcapsules of beta-carotene, depending on their relationship with carotenoid metabolism, all the enriched terms can be divided into the following three categories: a. terms directly correlated with metabolism of carotenoids and their derivatives (absorption, transport and metabolic transformation); b. terms relating to fat metabolism; c. terms regarding transcription factors (Table S6).

Notably, three down-regulated genes (LOC117684251, LOC105348216, LOC105341121) encoding carotenoid cleavage enzymes were enriched in the pathway of retinol metabolism, among which the latter two genes encode identical protein sequences. DEGs included in this pathway are marked in the pathway map (map00830) (Fig. 5). Among those, retinol dehydrogenase 8 (RDH) and UGT (glucuronosyltransferase) were also down-regulated in group caro, whereas some members of cytochrome P450 family were up-regulated. In addition, in the pathway of vitamin digestion and absorption, apolipoprotein genes (LOC105342035 and LOC105342186), known as the main chylomicron apoproteins, were upregulated. In terms of PPAR signaling pathway, LOC105323212 (peroxisome proliferator-activated receptor delta), LOC105331182 (nuclear receptor ROR-beta) and LOC117682968 were up regulated, together with a few of their downstream genes involved in lipid metabolism.

3.4. Sequence and phylogenetic analyses

The mRNA sequences of *CgApo1* and *CgApo2* were 15715 bp and 3060 bp in length, with ORFs encoding 5373 and 886 aa, respectively. The predicted amino acid sequences of these two *CgApo* genes both contain the LPD-N domain (Fig. 1a). Furthermore, LOC105323212, LOC105331182 and LOC117682968 (only containing LBD) were found to contain characteristic domains, i.e., DNA binding domain (DBD) and ligand binding domain (LBD), compatible with the role of nuclear receptors (Fig. 1b).

Conserved domains of amino acid sequences encoded by *CgApo1* and *CgApo2* were aligned with their known homologous genes in other species using MAFFT (Fig. S6). We found a high degree of similarity among these sequences. Phylogenetic analysis revealed that *C. gigas* Apo-1 and Apo-2 were close to each other and clustered with the apolipoprotein gene of *Hyriopsis cumingii* with a support of 100% (Fig. 6a).

Through BLASTP we found 5 carotenoid oxygenases in *C. gigas*, and

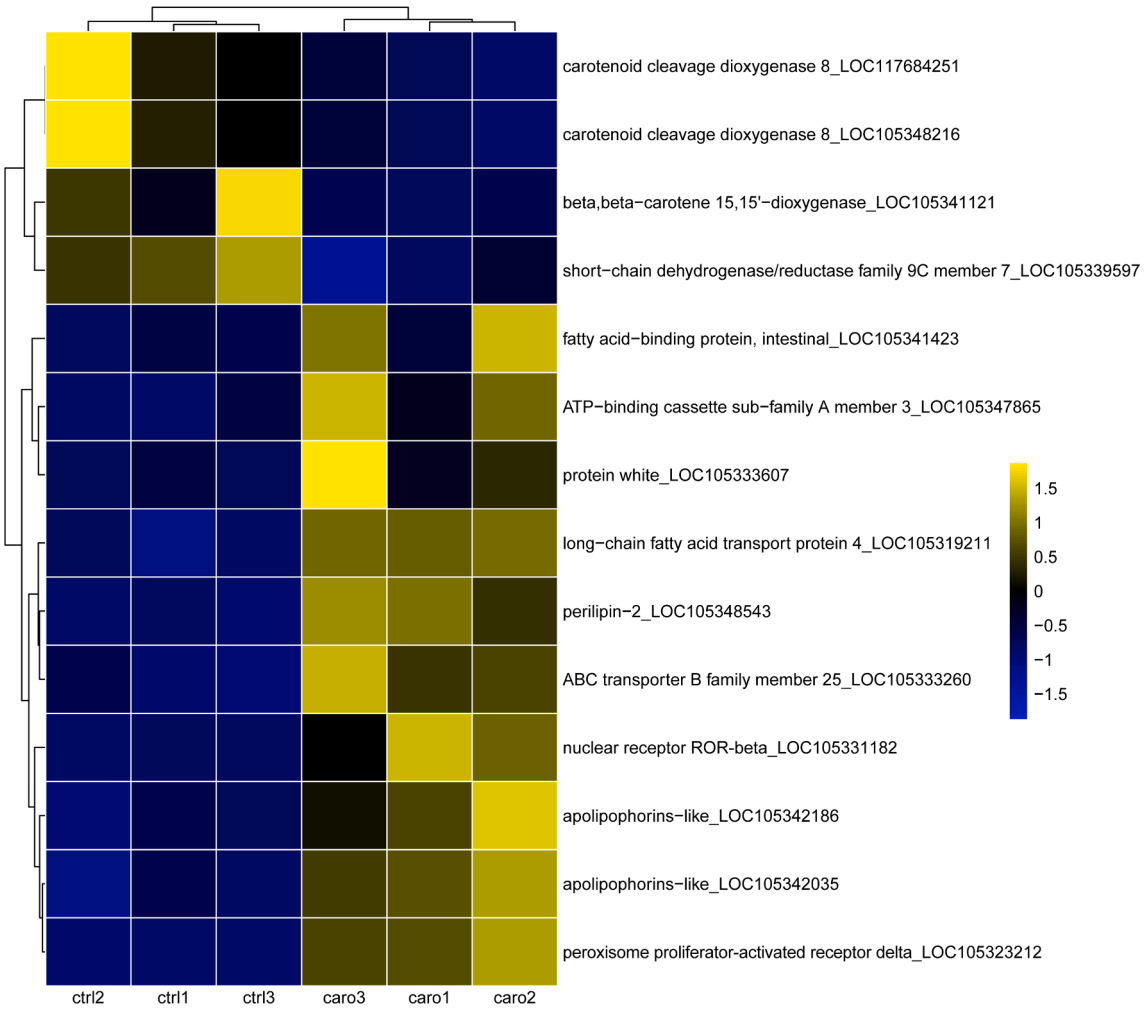

Fig. 2. Heatmap showing differential expression of representative genes between the beta-carotene supplemented group and control group. Yellow and blue shadings represent higher and lower relative expression levels, respectively. (For interpretation of the references to color in this figure legend, the reader is referred to the web version of this article.)

three were downregulated in group caro. Similar sequence and phylogenetic analyses performed on carotenoid oxygenases showed that their conserved domains share a high degree of similarity (39.58–65.62%), but the existence of slight differences may be associated with the substrate specificity (Fig. S7a). Among those, proteins of LOC105321989 and LOC117690758, as well as LOC117684251 and LOC105348216 were identical to each other respectively (Fig. S7a), which may result from gene duplication event, and we have to take the mRNAs of two identical genes as one target of qPCR. Phylogenetic analysis demonstrated that the protein of LOC105341121 is close to BCOlike 1 in Yesso scallop and they group together with other *C. gigas* carotenoid oxygenases with a with a support of 100% (Fig. S7b).

3.5. mRNA expressions of CgApo genes and carotenoid content in the digestive gland after RNAi

To identify the role of *CgApo1* and *CgApo2* in carotenoid metabolism, we synthesized the dsRNA (dsApo) and injected them into oyster adductor muscle at 100 μg twice for each individual.

Results of qRT-PCR showed that the mRNA expression levels of *CgApo1* and *CgApo2* in the digestive gland were inhibited after RNAi. The expression levels of *CgApo1* and *CgApo2* mRNA were about 46.47–78.05% downregulated compared with the dsEGFP and PBS injected groups (Fig. 6b,c). Furthermore, significant expression differences were found between the RNAi group and PBS group of both *CgApo* genes. Even though the differences between RNAi group and EGFP group were not significant, expression of *CgApo* genes were roughly lower in the RNAi group.

After the RNAi experiment, total carotenoid content (TCC) in the digestive gland of *C. gigas* was determined. The results showed that TCC of the dsApo group is lower than that of dsEGFP ($P < 0.01$) and PBS ($P < 0.05$) group (Fig. 6d), suggesting that downregulation of *CgApo* genes suppressed the carotenoid accumulation in the digestive gland of *C. gigas*.

4. Discussion

4.1. Roles of the digestive gland in carotenoid processing of the Pacific oyster

In the present study, the transcriptome comparison between the digestive glands of oysters on a beta-carotene supplemented diet and a normal diet identified a set of 718 DEGs, many of which are associated with lipid transport and storage, carotenoid processing and retinol metabolism.

Mollusks contain a wide range of structurally different carotenoids obtained from their dietary microalgae (Maoka, 2011), rely on steps of absorption, transport, metabolism and deposition implemented by various genes (Parker, 1996). These steps are considered to mainly happen in the digestive gland as high carotenoid content was found in

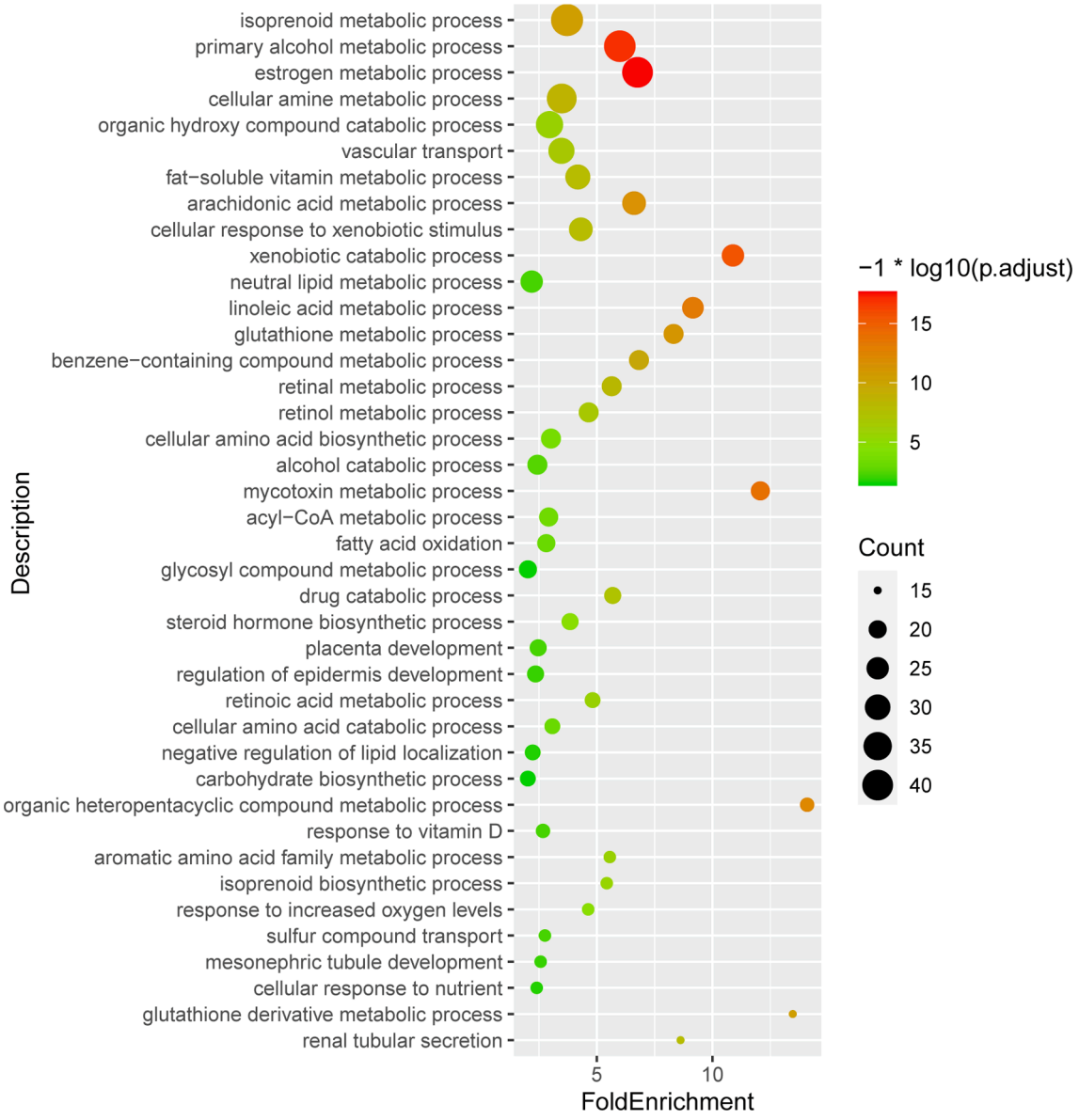

Fig. 3. Enriched GO terms related to DEGs in the Biological Process category at level 5.

the hepatopancreas of most freshwater species (Vershinin, 1996). Indeed, it has been well established that certain specialized cells in the digestive gland of mollusks perform multiple tasks including digestion of small molecules, transport of nutrients, and storage of lipid droplets that may be rich in carotenoids. In particular, it should be noted that the storage function was found for the digestive tract epithelial-supporting cells of mollusks, in contrast to vertebrate cells whose primary function is not intracellular digestion and storage (Lobo-da-Cunha, 2019).

In *C. gigas*, research has revealed the homology, functional similarity and evolutionary connections between oyster and vertebrate digestive tissues (Xu et al., 2021). Especially, transcriptomic comparison between the oyster digestive gland (mainly composed of hepatopancreas and few gut tissues) and other tissues demonstrated that hepatopancreas-enriched genes are compatible with a digestive role and encode digestive enzymes homologous to those produced by vertebrate pancreas. Actually, the vertebrate liver and intestine have been well characterized as important sites for genes to perform carotenoid-related functions such as carotenoid cleavage of CCOs (Raghuvanshi et al., 2015; Widjaja-Adhi et al., 2015) as well as transport and absorption of carotenoids of SRBs (Widjaja-Adhi et al., 2015), which leads us to reasonably speculate that the oyster digestive gland has a similar role.

In the following, we discuss the DEGs which might be associated with different cellular and metabolic processes regarding carotenoid processing.

4.2. *Functions of apolipoprotein in carotenoid transport and storage*

Apolipoprotein (Apo) was known to play an essential role in the assembly of lipoproteins functioning in the transport and storage of lipids, fat-soluble vitamins and carotenoids (Arrese et al., 2001; Weers and Ryan, 2006). The lipoproteins (including lipophorins in insects) formed may be bound by SRB to promote possibly selective uptake of lipids containing specific species of carotenoids (Kiefer et al., 2002; van Bennekum et al., 2005; Sakudoh et al., 2010).

Through comparative transcriptome analysis, qRT-PCR analyses and functional verifications, we identified two *C. gigas* Apo genes (NCBI accession: LOC105342035 and LOC105342186), designated *CgApo1* and *CgApo2* respectively, which may facilitate carotenoid storage. Multiple alignments showed that although CgApo1 (5373 aa) protein is much longer than and CgApo2 (886 aa), they share high sequence

Fig. 4. Enriched KEGG pathways related to all DEGs.

identity in the overlap region and both contain a lipoprotein N-terminal domain (LPD-N), a conserved feature of the large lipid transfer protein (LLTP) that may function as a recognition motif by lipoproteins (Avarre et al., 2007; Hayward et al., 2010). Notably, a high degree of sequence identity was observed between the CgApo and hcApo of the fresh-water pearl mussel *Hyriopsis cumingii*, which clustered on the same branch in the phylogenetic tree (Fig. 6a) constructed from their conserved domains, and could be grouped into the Apo subset containing homologs of other species. In fact, significantly positive correlation between the hcApo gene expression level and the total carotenoid content has been demonstrated in purple line pearl mussels (Li et al., 2014). Consistently, in the present study, RNAi of *CgApo* genes that downregulated the expression of *CgApo1* and *CgApo2* caused the decrease of TCC in the digestive gland of oysters, indicating that inhibition of *CgApo* may hinder lipoprotein assembly and thus carotenoid transport and storage. Similarly, consistent results of RNA-seq analyses in various tissues of *C. gigas* showed that apolipophorins-like (LOC105333749), which has 100% identity with CgApo2, was uniquely highly expressed in the digestive gland and constitutively expressed in other tissues (Zhang et al., 2012; Xu et al., 2021).

4.3. Negative feedback regulation of carotenoid cleavage and retinoid homeostasis

Expansion of carotenoid oxygenase genes in *C. gigas*, including a relatively independent gene (LOC105341121) and two groups of duplicated genes (i.e., LOC105321989 and LOC117690758; LOC105348216 and LOC117684251) may reflect complex interactions with the environment during evolution (Poliakov et al., 2017). Among these genes, three carotenoid cleavage oxygenases (CCOs) (LOC105341121, LOC105348216, LOC117684251) were down-regulated in group caro compared to group ctrl in our study, indicating that these genes may be associated with the ability of *C. gigas* to adapt to excessive carotenoids and excessive derived retinoids (including vitamin A, retinoic acid, and so on) (von Lintig, 2010). Notably, the expression of two carotenoid oxygenase genes (LOC105321989 and LOC117690758) was not altered, probably due to differences in their substrate specificity.

In vertebrates, CCOs can be classified into three classes (BCO1, BCO2 and RPE65) with different substrate specificity and cleavage manner (Hessel et al., 2007; Amengual et al., 2011). Furthermore, it is well established that BCO1 activity is under negative feedback regulation of

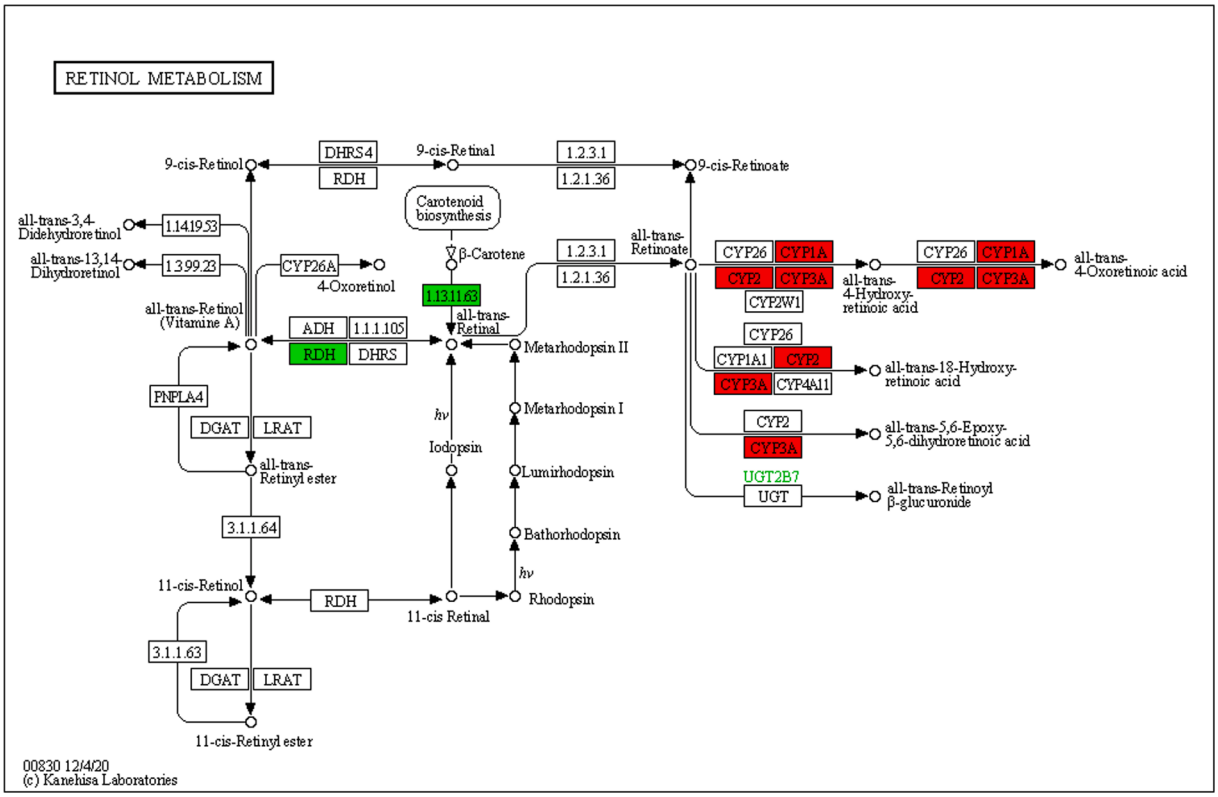

Fig 5. The Retinol metabolism pathway significantly enriched from the KEGG databse. Genes with green background were downregulated in group caro, and genes with red background were up-regulated in group caro compared with group ctrl. (For interpretation of the references to color in this figure legend, the reader is referred to the web version of this article.)

vitamin A, involving transcription factor genes RAR, RXR, PPAR and ISX (van Vliet et al., 1996; Seino et al., 2008; Lobo et al., 2013; Widjaja-Adhi et al., 2015). In comparison, among invertebrates, a BCO2-like (BCOL) clade exists, which includes lancelet, nematode, and molluscan carotenoid oxygenases with the activity demonstrated (Poliakov et al., 2017). Furthermore, there are a large number of homologs of nuclear receptor transcription factors in invertebrates playing crucial biological, developmental and reproductive processes (Vogeler et al., 2014). However, few reports have focused on whether invertebrate carotenoid cleavage oxygenases are subject to negative feedback regulation controlled by NRs.

In mollusks, through a combination of genomic approaches and functional assays, Li et al. (2019) showed a carotenoid oxygenase PyBCO-like 1 is capable of degrading beta-carotene and its down-regulation is responsible the carotenoid-based color of orange-muscle Yesso scallops compared with white-muscle ones (Li et al., 2019). Additionally, RAR and RXR genes have been reported to play possible roles in carotenoid metabolism by regulate SRB and BCO gene in noble scallop *Chlamys nobilis* rich in carotenoids (Tan et al., 2021b) (Tan et al., 2021a), compatible with the pattern mentioned above.

Interestingly, we found elevated expression of three nuclear receptor (NR) transcription factors (Fig. 1b), which may be responsible for the downregulation of three among five carotenoid cleavage oxygenases in *C. gigas*. Among them, we highlighted LOC105323212, annotated as "peroxisome proliferator-activated receptor delta" in NCBI, may form a heterodimer with RXR that can interact with ligands belonging to carotenoid derivatives (Vogeler et al., 2017).

Here, we put forward a hypothesis that a negative feedback regulation of retinoid homeostasis exists in the oyster, in which nuclear receptor transcription factors may regulate gene expressions of carotenoid cleavage oxygenases to control the conversion of carotenoids and retinoid production. This regulation may prevent excessive production of vitamin A when the supply of provitamin A carotenoids is abundant and promote its production in deficient conditions. Further experiments were needed to verify this hypothesis.

Importantly, a retinol dehydrogenase (RDH, LOC105339597) was downregulated in the group caro. RDH may play a key role in the interconversion of retinol to retinal and is an essential component of the regulation mechanism of retinoid homeostasis (Napoli, 2012; Kedishvili, 2013). Subsequently, the levels of ligands such as retinoic acid are regulated, whereby the activity of corresponding transcription factors is controlled for a wide range of processes such as cell differentiation, immunity, and metabolism (Blaner, 2019). In addition, other DEGs such as cytochrome P450 genes (LOC105343044, LOC105344043, LOC105337485), upregulated in group caro, may also play roles in carotenoid metabolism and retinoid homeostasis. For instance, a cytochrome P450 gene cluster in zebra finch (*Taeniopygia guttata*) contains candidates for the carotenoid ketolase, which catalyzes carotenoid ketolation (Mundy et al., 2016), and in mammals cytochrome P450 enzymes were responsible for RA degradation (Napoli, 2017). Notably, although the beta-carotene contained in microcapsules is potent, as evidenced by the expression changes of carotenoid cleavage oxygenases, shells of beta-carotene microcapsules containing triglyceride oil and surface active materials may act as interference factors, in the absence of a control group supplied with only shell substances to clear up these effects. For example, surface active materials may play a role as xenobiotics inducing detoxification response in oysters, which also involves cytochrome P450 genes. Therefore, the link between cytochrome P450 genes and carotenoid metabolism in Pacific oyster should be further investigated. Similarly, several additional DEGs in this study, such as perilipin gene (LOC105348543), involved in fatty acid metabolism, may also be affected by the triglyceride oil in the microcapsule shell (Granneman et al., 2017; Lin et al., 2018), and thus whether their functions are related to carotenoids needs to be further verified.

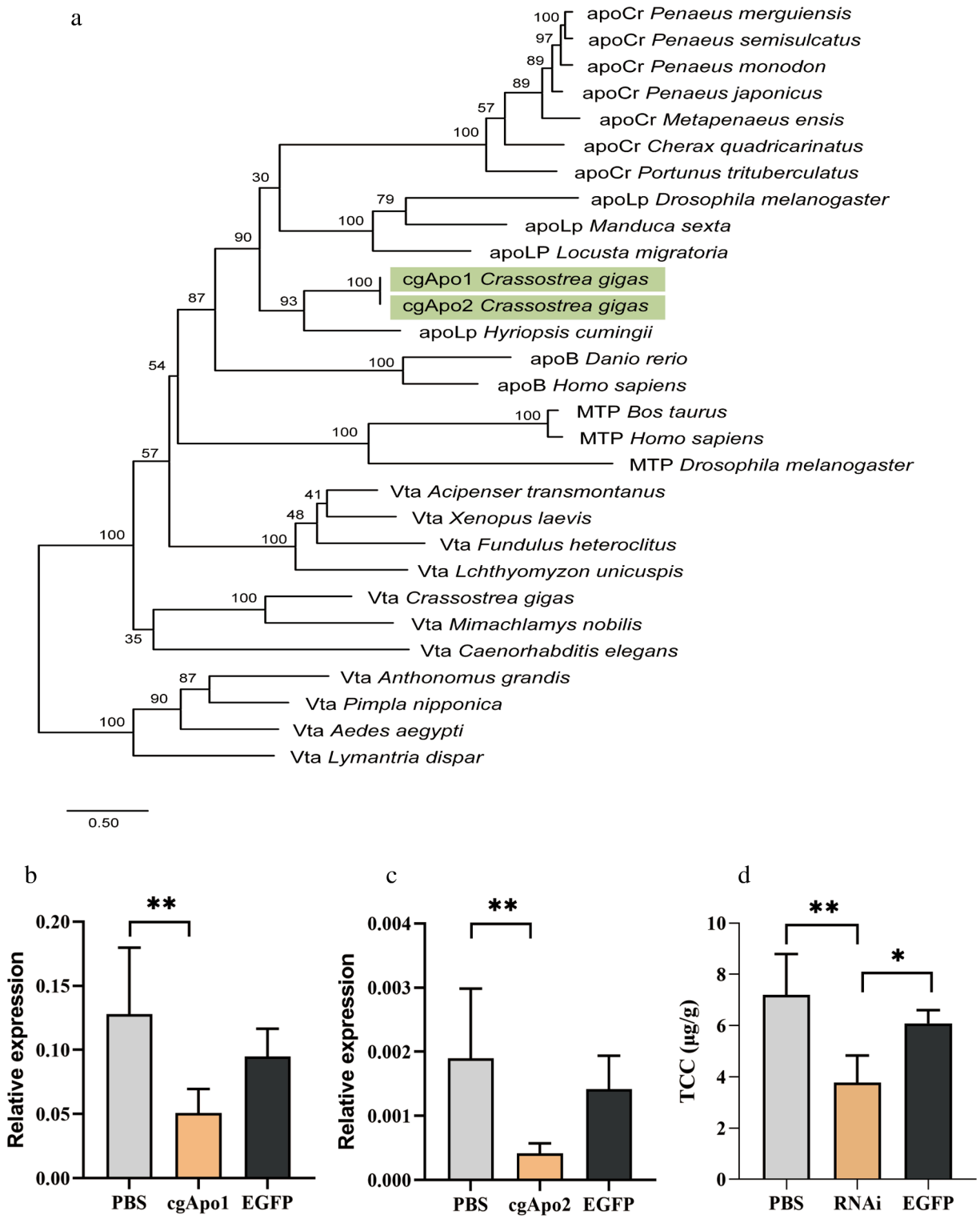

Fig. 6. a. A phylogenetic tree of apolipoprotein homologs among various phyla was constructed by Maximum Likelihood. The alignment was constructed using the lipoprotein N-terminal domain (LPD-N). Maximum Likelihood bootstrap support values (percentage of 1000 BS) are provided above the nodes. Protein sequences from Pimpla nipponica, Anthonomus grandis, Aedes aegypti and Lymantria dispar are used as an outgroup. The protein sequences with accession numbers are listed in S2 file. b. and c. CgApo1 and CgApo2 expressions were inhibited by dsRNA in the the RNAi group (CgApo1 and CgApo2) compared to the control groups (PBS and EGFP), according to the results of qPCR. d. Total carotenoid content (TCC) were lower in the RNAi group (CgApo), compared to the control groups (PBS and EGFP). $^{*}P < 0.05$, $^{**}P < 0.01$.

5. Conclusion

Taken together, we analyzed differential gene expression related to carotenoid metabolism based on a comparative analysis between oysters on a beta-carotene supplemented diet or a normal diet. Several induced differentially expressed genes possibly related to carotenoid metabolism were obtained, including two apolipoprotein genes, three carotenoid oxygenase genes, three nuclear receptor transcription factors, and a

retinol dehydrogenase. Results of functional assays provided support for the role of the two apolipoprotein genes in carotenoid transport and storage. We further proposed a negative feedback regulatory mechanism for retinoid production by carotenoid cleavage, including nuclear receptor transcription factors and possibly regulated downstream carotenoid oxygenase genes. Our findings provide useful information for potential mechanisms on molluscan carotenoid metabolism and point out several promising candidate genes for further study.

CRediT authorship contribution statement

Sai Wan: Writing – original draft, Methodology, Software. **Qi Li:** Supervision, Writing – review & editing. **Hong Yu:** Resources. **Shikai Liu:** Project administration. **Lingfeng Kong:** Resources.

Declaration of Competing Interest

The authors declare that they have no known competing financial interests or personal relationships that could have appeared to influence the work reported in this paper.

Acknowledgements

This work was supported by the grants from National Natural Science Foundation of China (31972789 and 31772843), Earmarked Fund for Agriculture Seed Improvement Project of Shandong Province (2020LZGC016), and Industrial Development Project of Qingdao City (20-3-4-16-nsh).

Appendix A. Supplementary material

Supplementary data to this article can be found online at https://doi.org/10.1016/j.gene.2022.146226.

References

Amengual, J., Lobo, G.P., Golczak, M., Li, H.N., Klimova, T., Hoppel, C.L., Wyss, A., Palczewski, K., von Lintig, J., 2011. A mitochondrial enzyme degrades carotenoids and protects against oxidative stress. FASEB J. 25, 948–959.

Andre, A., Ruivo, R., Gesto, M., Castro, L.F., Santos, M.M., 2014. Retinoid metabolism in invertebrates: when evolution meets endocrine disruption. Gen. Comp. Endocrinol. 208, 134–145.

Arrese, E.L., Canavoso, L.E., Jouni, Z.E., Pennington, J.E., Tsuchida, K., Wells, M.A., 2001. Lipid storage and mobilization in insects: current status and future directions. Insect Biochem. Mol. Biol. 31, 7–17.

Avarre, J.C., Lubzens, E., Babin, P.J., 2007. Apolipocrustacein, formerly vitellogenin, is the major egg yolk precursor protein in decapod crustaceans and is homologous to insect apolipophorin II/I and vertebrate apolipoprotein B. BMC Evol. Biol. 7, 3.

Blaner, W.S., 2019. Vitamin A signaling and homeostasis in obesity, diabetes, and metabolic disorders. Pharmacol. Ther. 197, 153–178.

Boulanger, A., McLemore, P., Copeland, N.G., Gilbert, D.J., Jenkins, N.A., Yu, S.S., Gentleman, S., Redmond, T.M., 2003. Identification of beta-carotene 15, 15'-monooxygenase as a peroxisome proliferator-activated receptor target gene. FASEB J. 17, 1304–1306.

Chen, S., Zhou, Y., Chen, Y., Gu, J., 2018. fastp: an ultra-fast all-in-one FASTQ preprocessor. Bioinformatics 34, i884–i890.

Chen, X., Bai, Z., Li, J., 2019. The Mantle Exosome and MicroRNAs of Hyriopsis cumingii Involved in Nacre Color Formation. Mar. Biotechnol. 21, 634–642.

Chimsung, N., Lall, S.P., Tantikitti, C., Verlhac-Trichet, V., Milley, J.E., 2013. Effects of dietary cholesterol on astaxanthin transport in plasma of Atlantic salmon (Salmo salar). Comp. Biochem. Phys. B 165, 73–81.

During, A., Dawson, H.D., Harrison, E.H., 2005. Carotenoid transport is decreased and expression of the lipid transporters SR-BI, NPC1L1, and ABCA1 is downregulated in Caco-2 cells treated with ezetimibe. J. Nutr. 135, 2305–2312.

Eriksson, J., Larson, G., Gunnarsson, U., Bed'hom, B., Tixier-Boichard, M., Stromstedt, L., Wright, D., Jungerius, A., Vereijken, A., Randi, E., Jensen, P., Andersson, L., 2008. Identification of the yellow skin gene reveals a hybrid origin of the domestic chicken. PLoS Genet. 4, e1000010.

FAO, 2016. The State of World Fisheries and Aquaculture, Food and Agriculture Organization of the United Nations, Rome, Italy.

Granneman, J.G., Kimler, V.A., Zhang, H., Ye, X., Luo, X., Postlethwait, J.H., Thummel, R., 2017. Lipid droplet biology and evolution illuminated by the characterization of a novel perilipin in teleost fish. Elife 6.

Hall, J.A., Grainger, J.R., Spencer, S.P., Belkaid, Y., 2011. The role of retinoic acid in tolerance and immunity. Immunity 35, 13–22.

Hayward, A., Takahashi, T., Bendena, W.G., Tobe, S.S., Hui, J.H., 2010. Comparative genomic and phylogenetic analysis of vitellogenin and other large lipid transfer proteins in metazoans. FEBS Lett. 584, 1273–1278.

Herron, K.L., McGrane, M.M., Waters, D., Lofgren, I.E., Clark, R.M., Ordovas, J.M., Fernandez, M.L., 2006. The ABCG5 polymorphism contributes to individual responses to dietary cholesterol and carotenoids in eggs. J. Nutr. 136, 1161–1165.

Hessel, S., Eichinger, A., Isken, A., Amengual, J., Hunzelmann, S., Hoeller, U., Elste, V., Hunziker, W., Goralczyk, R., Oberhauser, V., von Lintig, J., Wyss, A., 2007. CMO1 deficiency abolishes vitamin A production from beta-carotene and alters lipid metabolism in mice. J. Biol. Chem. 282, 33553–33561.

Hubbard, J.K., Uy, J.A., Hauber, M.E., Hoekstra, H.E., Safran, R.J., 2010. Vertebrate pigmentation: from underlying genes to adaptive function. Trends Genet. 26, 231–239.

Kanehisa, M., Araki, M., Goto, S., Hattori, M., Hirakawa, M., Itoh, M., Katayama, T., Kawashima, S., Okuda, S., Tokimatsu, T., Yamanishi, Y., 2008. KEGG for linking genomes to life and the environment. Nucleic. Acids. Res. 36, D480–D484.

Katoh, K., Misawa, K., Kuma, K., Miyata, T., 2002. MAFFT: a novel method for rapid multiple sequence alignment based on fast Fourier transform. Nucleic Acids Res. 30, 3059–3066.

Kedishvili, N.Y., 2013. Enzymology of retinoic acid biosynthesis and degradation. J. Lipid. Res. 54, 1744–1760.

Khatri, P., Draghici, S., 2005. Ontological analysis of gene expression data: current tools, limitations, and open problems. Bioinformatics 21, 3587–3595.

Kiefer, C., Sumser, E., Wernet, M.F., Von Lintig, J., 2002. A class B scavenger receptor mediates the cellular uptake of carotenoids in Drosophila. Proc. Natl. Acad. Sci. USA 99, 10581–10586.

Kim, D., Langmead, B., Salzberg, S.L., 2015. HISAT: a fast spliced aligner with low memory requirements. Nat. Methods 12, 357–360.

Kiser, P.D., Golczak, M., Palczewski, K., 2014. Chemistry of the retinoid (visual) cycle. Chem. Rev. 114, 194–232.

Kuhn, D.D., Angier, M.W., Barbour, S.L., Smith, S.A., Flick, G.J., 2013. Culture feasibility of eastern oysters (Crassostrea virginica) in zero-water exchange recirculating aquaculture systems using synthetically derived seawater and live feeds. Aquacult. Eng. 54, 45–48.

Letunic, I., Khedkar, S., Bork, P., 2021. SMART: recent updates, new developments and status in 2020. Nucleic Acids Res. 49, D458–D460.

Li, H., Handsaker, B., Wysoker, A., Fennell, T., Ruan, J., Homer, N., Marth, G., Abecasis, G., Durbin, R., Genome Project Data Processing, S., 2009. The Sequence Alignment/Map format and SAMtools. Bioinformatics 25, 2078–2079.

Li, L., Xue, C., Zhang, T., Wang, Y., 2020. The interaction between dietary marine components and intestinal flora. Mar Life Sci. Technol. 2, 161–171.

Li, N., Hu, J.J., Wang, S., Cheng, J., Hu, X.L., Lu, Z.Y., Lin, Z.J., Zhu, W.M., Bao, Z.M., 2010. Isolation and identification of the main carotenoid pigment from the rare orange muscle of the Yesso scallop. Food Chem. 118, 616–619.

Li, X., Bai, Z., Luo, H., Liu, Y., Wang, G., Li, J., 2014. Cloning, differential tissue expression of a novel hcApo gene, and its correlation with total carotenoid content in purple and white inner-shell color pearl mussel Hyriopsis cumingii. Gene 538, 258–265.

Li, X., Ning, X., Dou, J., Yu, Q., Wang, S., Zhang, L., Wang, S., Hu, X., Bao, Z., 2015. An SCD gene from the Mollusca and its upregulation in carotenoid-enriched scallops. Gene 564, 101–108.

Li, X., Wang, S., Xun, X., Zhang, M., Wang, S., Li, H., Zhao, L., Fu, Q., Wang, H., Li, T., Lian, S., Xing, Q., Li, X., Wu, W., Zhang, L., Hu, X., Bao, Z., 2019. A carotenoid oxygenase is responsible for muscle coloration in scallop. BBA-Mol. Cell Biol. Lipids 1864, 966–975.

Lin, Q., Liang, R., Williams, P.A., Zhong, F., 2018. Factors affecting the bioaccessibility of β-carotene in lipid-based microcapsules: Digestive conditions, the composition, structure and physical state of microcapsules. Food Hydrocolloids 77, 187–203.

Liu, H., Zheng, H., Zhang, H., Deng, L., Liu, W., Wang, S., Meng, F., Wang, Y., Guo, Z., Li, S., Zhang, G., 2015. A de novo transcriptome of the noble scallop, Chlamys nobilis, focusing on mining transcripts for carotenoid-based coloration. BMC Genom. 16, 44.

Lobo-da-Cunha, A., 2019. Structure and function of the digestive system in molluscs. Cell Tissue Res. 377, 475–503.

Lobo, G.P., Amengual, J., Baus, D., Shivdasani, R.A., Taylor, D., von Lintig, J., 2013. Genetics and diet regulate vitamin A production via the homeobox transcription factor ISX. J. Biol. Chem. 288, 9017–9027.

Lobo, G.P., Hessel, S., Eichinger, A., Noy, N., Moise, A.R., Wyss, A., Palczewski, K., von Lintig, J., 2010. ISX is a retinoic acid-sensitive gatekeeper that controls intestinal beta, beta-carotene absorption and vitamin A production. FASEB J. 24, 1656–1666.

Lopes, R.J., Johnson, J.D., Toomey, M.B., Ferreira, M.S., Araujo, P.M., Melo-Ferreira, J., Andersson, L., Hill, G.E., Corbo, J.C., Carneiro, M., 2016. Genetic Basis for Red Coloration in Birds. Curr. Biol. 26, 1427–1434.

Malerød, L., Sporstøl, M., Juvet, L.K., Mousavi, A., Gjøen, T., Berg, T., 2003. Hepatic scavenger receptor class B, type I is stimulated by peroxisome proliferator-activated receptor γ and hepatocyte nuclear factor 4α. Biochem. Bioph. Res. Co. 305, 557–565.

Maoka, T., 2009. Recent progress in structural studies of carotenoids in animals and plants. Arch. Biochem. Biophys. 483, 191–195.

Maoka, T., 2011. Carotenoids in marine animals. Mar. Drugs 9, 278–293.

Minh, B.Q., Nguyen, M.A., von Haeseler, A., 2013. Ultrafast approximation for phylogenetic bootstrap. Mol. Biol. Evol. 30, 1188–1195.

Moran, N.A., Jarvik, T., 2010. Lateral transfer of genes from fungi underlies carotenoid production in aphids. Science 328, 624–627.

Mundy, N.I., Stapley, J., Bennison, C., Tucker, R., Twyman, H., Kim, K.W., Burke, T., Birkhead, T.R., Andersson, S., Slate, J., 2016. Red Carotenoid Coloration in the Zebra Finch Is Controlled by a Cytochrome P450 Gene Cluster. Curr. Biol. 26, 1435–1440.

Napoli, J.L., 2012. Physiological insights into all-trans-retinoic acid biosynthesis. Biochim. Biophys. Acta 1821, 152–167.
Napoli, J.L., 2017. Cellular retinoid binding-proteins, CRBP, CRABP, FABP5: Effects on retinoid metabolism, function and related diseases. Pharmacol. Ther. 173, 19–33.
Olsen, R.E., Kiessling, A., Milley, J.E., Ross, N.W., Lall, S.P., 2005. Effect of lipid source and bile salts in diet of Atlantic salmon, Salmo salar L., on astaxanthin blood levels. Aquaculture 250, 804–812.
Parker, R.S., 1996. Absorption, metabolism, and transport of carotenoids. FASEB J. 10, 542–551.
Pertea, M., Pertea, G.M., Antonescu, C.M., Chang, T.C., Mendell, J.T., Salzberg, S.L., 2015. StringTie enables improved reconstruction of a transcriptome from RNA-seq reads. Nat. Biotechnol. 33, 290–295.
Poliakov, E., Soucy, J., Gentleman, S., Rogozin, I.B., Redmond, T.M., 2017. Phylogenetic analysis of the metazoan carotenoid oxygenase superfamily: a new ancestral gene assemblage of BCO-like (BCOL) proteins. Sci. Rep. 7, 13192.
Raghuvanshi, S., Reed, V., Blaner, W.S., Harrison, E.H., 2015. Cellular localization of beta-carotene 15,15' oxygenase-1 (BCO1) and beta-carotene 9',10' oxygenase-2 (BCO2) in rat liver and intestine. Arch. Biochem. Biophys. 572, 19–27.
Renault, T., Faury, N., Barbosa-Solomieu, V., Moreau, K., 2011. Suppression substractive hybridisation (SSH) and real time PCR reveal differential gene expression in the Pacific cupped oyster, Crassostrea gigas, challenged with Ostreid herpesvirus 1. Dev. Comp. Immunol. 35, 725–735.
Sakudoh, T., Iizuka, T., Narukawa, J., Sezutsu, H., Kobayashi, I., Kuwazaki, S., Banno, Y., Kitamura, A., Sugiyama, H., Takada, N., Fujimoto, H., Kadono-Okuda, K., Mita, K., Tamura, T., Yamamoto, K., Tsuchida, K., 2010. A CD36-related transmembrane protein is coordinated with an intracellular lipid-binding protein in selective carotenoid transport for cocoon coloration. J. Biol. Chem. 285, 7739–7751.
Sakudoh, T., Kuwazaki, S., Iizuka, T., Narukawa, J., Yamamoto, K., Uchino, K., Sezutsu, H., Banno, Y., Tsuchida, K., 2013. CD36 homolog divergence is responsible for the selectivity of carotenoid species migration to the silk gland of the silkworm Bombyx mori. J. Lipid. Res. 54, 482–495.
Seino, Y., Miki, T., Kiyonari, H., Abe, T., Fujimoto, W., Kimura, K., Takeuchi, A., Takahashi, Y., Oiso, Y., Iwanaga, T., Seino, S., 2008. Isx participates in the maintenance of vitamin A metabolism by regulation of beta-carotene 15,15'-monooxygenase (Bcmo1) expression. J. Biol. Chem. 283, 4905–4911.
Shahidi, F., Metusalach, Brown, J.A., 1998. Carotenoid pigments in seafoods and aquaculture. Crit. Rev. Food Sci. Nutr. 38, 1–67.
Song, J., Wang, C., 2019. Transcriptomic and proteomic analyses of genetic factors influencing adductor muscle coloration in QN Orange scallops. BMC Genom. 20, 363.
Tan, K., Deng, L.H., Zhang, H.K., Ma, H.Y., Li, S.K., Zheng, H.P., 2021a. Cloning and characterization of RARs and RXRs from noble scallop Chlamys nobilis, a bivalve rich in carotenoids. Aquac. Res.
Tan, K., Guo, Z.C., Zhang, H.K., Ma, H.Y., Li, S.K., Zheng, H.P., 2021b. Carotenoids regulation in polymorphic noble scallops Chlamys nobilis under different light cycle. Aquaculture 531, 735937.
Toews, D.P., Taylor, S.A., Vallender, R., Brelsford, A., Butcher, B.G., Messer, P.W., Lovette, I.J., 2016. Plumage Genes and Little Else Distinguish the Genomes of Hybridizing Warblers. Curr. Biol. 26, 2313–2318.
Toews, D.P.L., Hofmeister, N.R., Taylor, S.A., 2017. The Evolution and Genetics of Carotenoid Processing in Animals. Trends Genet. 33, 171–182.
Toomey, M.B., Lopes, R.J., Araujo, P.M., Johnson, J.D., Gazda, M.A., Afonso, S., Mota, P. G., Koch, R.E., Hill, G.E., Corbo, J.C., Carneiro, M., 2017. High-density lipoprotein receptor SCARB1 is required for carotenoid coloration in birds. Proc. Natl. Acad. Sci. USA 114, 5219–5224.
Twyman, H., Valenzuela, N., Literman, R., Andersson, S., Mundy, N.I., 2016. Seeing red to being red: conserved genetic mechanism for red cone oil droplets and co-option for red coloration in birds and turtles. Proc. Biol. Sci. 283.
van Bennekum, A., Werder, M., Thuahnai, S.T., Han, C.H., Duong, P., Williams, D.L., Wettstein, P., Schulthess, G., Phillips, M.C., Hauser, H., 2005. Class B scavenger receptor-mediated intestinal absorption of dietary beta-carotene and cholesterol. Biochemistry 44, 4517–4525.
van Vliet, T., van Vlissingen, M.F., van Schaik, F., van den Berg, H., 1996. beta-Carotene absorption and cleavage in rats is affected by the vitamin A concentration of the diet. J. Nutr. 126, 499–508.
Vershinin, A., 1996. Carotenoids in mollusca: Approaching the functions. Comp. Biochem. Phys. B 113, 63–71.
Vitting-Seerup, K., Sandelin, A., 2019. IsoformSwitchAnalyzeR: analysis of changes in genome-wide patterns of alternative splicing and its functional consequences. Bioinformatics 35, 4469–4471.
Vogeler, S., Galloway, T.S., Lyons, B.P., Bean, T.P., 2014. The nuclear receptor gene family in the Pacific oyster, *Crassostrea gigas*, contains a novel subfamily group. BMC Genom. 15, 369.
Vogeler, S., Galloway, T.S., Isupov, M., Bean, T.P., 2017. Cloning retinoid and peroxisome proliferator-activated nuclear receptors of the Pacific oyster and in silico binding to environmental chemicals. PLoS One 12, e0176024.
von Lintig, J., 2010. Colors with functions: elucidating the biochemical and molecular basis of carotenoid metabolism. Annu. Rev. Nutr. 30, 35–56.
Wang, L., Feng, Z., Wang, X., Wang, X., Zhang, X., 2010. DEGseq: an R package for identifying differentially expressed genes from RNA-seq data. Bioinformatics 26, 136–138.
Wang, S., Lv, J., Zhang, L., Dou, J., Sun, Y., Li, X., Fu, X., Dou, H., Mao, J., Hu, X., Bao, Z., 2015. MethylRAD: a simple and scalable method for genome-wide DNA methylation profiling using methylation-dependent restriction enzymes. Open Biol. 5.
Waterhouse, A.M., Procter, J.B., Martin, D.M., Clamp, M., Barton, G.J., 2009. Jalview Version 2–a multiple sequence alignment editor and analysis workbench. Bioinformatics 25, 1189–1191.
Weers, P.M., Ryan, R.O., 2006. Apolipophorin III: role model apolipoprotein. Insect Biochem. Mol. Biol. 36, 231–240.
Widjaja-Adhi, M.A., Lobo, G.P., Golczak, M., Von Lintig, J., 2015. A genetic dissection of intestinal fat-soluble vitamin and carotenoid absorption. Hum. Mol. Genet. 24, 3206–3219.
Xiao, J.H., Durand, B., Chambon, P., Voorhees, J.J., 1995. Endogenous retinoic acid receptor (RAR)-retinoid X receptor (RXR) heterodimers are the major functional forms regulating retinoid-responsive elements in adult human keratinocytes. Binding of ligands to RAR only is sufficient for RAR-RXR heterodimers to confer ligand-dependent activation of hRAR beta 2/RARE (DR5). J. Biol. Chem. 270, 3001–3011.
Xu, F., Marletaz, F., Gavriouchkina, D., Liu, X., Sauka-Spengler, T., Zhang, G., Holland, P. W.H., 2021. Evidence from oyster suggests an ancient role for Pdx in regulating insulin gene expression in animals. Nat. Commun. 12, 3117.
Xu, M., Huang, J., Shi, Y., Zhang, H., He, M., 2019. Comparative transcriptomic and proteomic analysis of yellow shell and black shell pearl oysters, Pinctada fucata martensii. BMC Genom. 20, 469.
Yabuzaki, J., 2017. Carotenoids Database: structures, chemical fingerprints and distribution among organisms. Database (Oxford) 2017.
Yanar, Y., Celik, M., Yanar, M., 2004. Seasonal changes in total carotenoid contents of wild marine shrimps (Penaeus semisulcatus and Metapenaeus monoceros) inhabiting the eastern Mediterranean. Food Chem. 88, 267–269.
Ye, J., Coulouris, G., Zaretskaya, I., Cutcutache, I., Rozen, S., Madden, T.L., 2012. Primer-BLAST: a tool to design target-specific primers for polymerase chain reaction. BMC Bioinformat. 13, 134.
Yu, G., Wang, L.G., Han, Y., He, Q.Y., 2012. clusterProfiler: an R package for comparing biological themes among gene clusters. OMICS 16, 284–287.
Yuan, H., Zhang, J., Nageswaran, D., Li, L., 2015. Carotenoid metabolism and regulation in horticultural crops. Hortic. Res. 2, 15036.
Zhang, G., Fang, X., Guo, X., Li, L., Luo, R., Xu, F., Yang, P., Zhang, L., Wang, X., Qi, H., Xiong, Z., Que, H., Xie, Y., Holland, P.W., Paps, J., Zhu, Y., Wu, F., Chen, Y., Wang, J., Peng, C., Meng, J., Yang, L., Liu, J., Wen, B., Zhang, N., Huang, Z., Zhu, Q., Feng, Y., Mount, A., Hedgecock, D., Xu, Z., Liu, Y., Domazet-Loso, T., Du, Y., Sun, X., Zhang, S., Liu, B., Cheng, P., Jiang, X., Li, J., Fan, D., Wang, W., Fu, W., Wang, T., Wang, B., Zhang, J., Peng, Z., Li, Y., Li, N., Wang, J., Chen, M., He, Y., Tan, F., Song, X., Zheng, Q., Huang, R., Yang, H., Du, X., Chen, L., Yang, M., Gaffney, P.M., Wang, S., Luo, L., She, Z., Ming, Y., Huang, W., Zhang, S., Huang, B., Zhang, Y., Qu, T., Ni, P., Miao, G., Wang, J., Wang, Q., Steinberg, C.E., Wang, H., Li, N., Qian, L., Zhang, G., Li, Y., Yang, H., Liu, X., Wang, J., Yin, Y., Wang, J., 2012. The oyster genome reveals stress adaptation and complexity of shell formation. Nature 490, 49–54.
Zhang, Y., Zhang, L., Sun, J., Qiu, J., Hu, X., Hu, J., Bao, Z., 2014. Proteomic analysis identifies proteins related to carotenoid accumulation in Yesso scallop (Patinopecten yessoensis). Food Chem. 147, 111–116.
Zhao, S., Fernald, R.D., 2005. Comprehensive algorithm for quantitative real-time polymerase chain reaction. J. Comput. Biol. 12, 1047–1064.